PHYSICAL REVIEW B VOLUME 19, NUMBER 8 15 APRIL 1979

Band limits and the vibrational spectra of tetrahedral glasses

Frank L. Galeener
Xerox Palo Alto Research Center, 3333 Coyote Hill Road, Palo Alto, California 94304
(Received 11 September 1978)

The primary features of the Raman and infrared spectra of AX_2 tetrahedral glasses are associated with the *edges* of the vibrational bands calculated by Sen and Thorpe. The dominant Raman peak is assigned to a singular *matrix element* rather than a peak in the density of vibrational states. Simple expressions are developed which yield useful values of the vibrational force constants and intertetrahedral angles for vitreous SiO_2, GeO_2, and BeF_2.

In this paper, I develop a method for analyzing the vibrational spectra of AX_2 tetrahedral glasses which is based on intepreting the vibrational-band limits previously calculated for a central-force network model by Sen and Thorpe (ST).[1] The method leads to simple formulas for the direct experimental determination of force constants and intertetrahedral angles to within 10% of the correct values.[2] The substantial computational simplification accomplished by this method is accompanied by new physical insight into the nature of the normal modes and the selection rules for these and other glasses.

I. CENTRAL-FORCE NETWORK MODEL

Figure 1 illustrates the local order assumed by ST. It shows two neighboring tetrahedra, drawn schematically in the AXA plane that involves the single shared X atom. This local topology is repeated throughout space: All A-X bond distances are the same, all X-A-X angles have the tetrahedral values $\cos^{-1}(-\frac{1}{3}) \simeq 109.5°$, and all intertetrahedral A-X-A angles have the common value θ. The symbols B, S, and R indicate "bending," "stretching," and "rocking" motions of the X atom, using a nomenclature first introduced by Bell and Dean.[3] The structure does not necessarily contain rings of bonds. It embodies certain elements of disorder, since it is *not* periodic in space and the dihedral angles may have any values. (A dihedral angle gives the orientation of an A-X-A plane relative to one of the tetrahedra that it links.)

Assuming that all force constants are zero except for the A-X bond-stretching constant α, ST obtained the following expressions for the spectral limits of the two highest-frequency bands in the density of vibrational states of such a system:

$$\omega_1^2 = (\alpha/m_X)(1+\cos\theta)\,, \tag{1}$$

$$\omega_2^2 = (\alpha/m_X)(1-\cos\theta)\,, \tag{2}$$

$$\omega_2^2 = \omega_1^2 + (4\alpha/3m_A)\,, \tag{3}$$

$$\omega_2^2 = \omega_2^2 + 4\alpha/3m_A\,. \tag{4}$$

Here, ω_i are angular frequencies (rad/sec), while m_X and m_A are the mass of the X and A atom. [All equations in this paper remain true if we replace ω by the wave-number value W (cm^{-1}) of the frequency, m by the atomic weight M of the atom, and α by $\alpha/0.0593$, where $\alpha = \alpha$ (dyn/cm) $= 10^3\alpha$ (N/m).] The dependence of these expressions on intertetrahedral angle θ is illustrated by the solid lines in Fig. 2, for the special case α

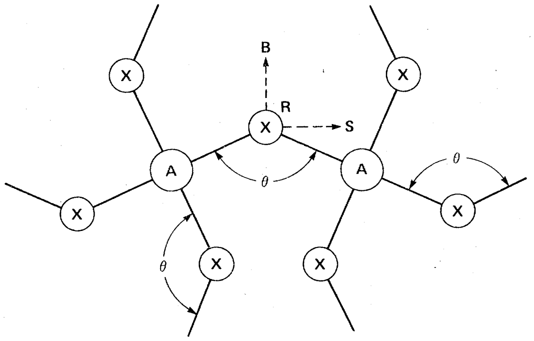

FIG. 1. Schematic diagram of local order assumed for tetrahedral AX_2 glass, showing common intertetrahedral angle θ.

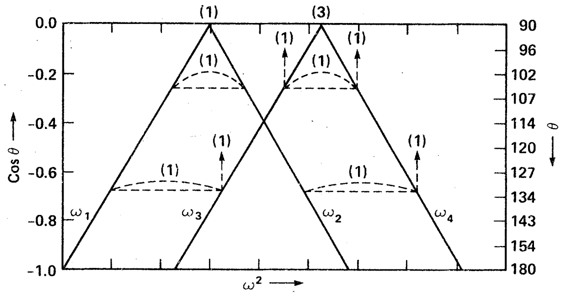

FIG. 2. Diagram of Eqs. (1)–(4) showing dependence of band edges on intertetrahedral angle θ. The dashed lines are a schematic of the density of states at two different values of θ, with relative weights given in parentheses.

independent of θ.

It is important to understand the relation of θ to the frequency distribution of the bands calculated by ST. The dashed lines in Fig. 2 are a *schematic* representation of the density of vibrational states for two different values of θ, one above the crossover angle $\theta_c = \cos^{-1}(-2m_X/3m_A)$ and one below. The relative weights in the density of states are given in parentheses, with vertical arrows indicating δ functions of unit area. These states account for four of the nine expected per formula unit AX_2; the others are driven to zero by their acoustic nature, and by the assumption that the noncentral force constant β is zero. When $\theta = 90°$, the tetrahedral units are effectively uncoupled, and the frequencies are the same as those of an isolated tetrahedral molecule having no bond-bending restoring forces, i.e., having bond-stretching forces *only*. For example, ω_1 (90°) is the frequency of the nondegenerate (A_1) "breathing" mode of such a molecule, while ω_3 (90°) is the frequency of the threefold-degenerate (F_2) "rigid cage" mode. As θ increases above 90°, the situation changes drastically from that expected for isolated molecules. The A_1 mode broadens into a band of states having unit-normalized area, while the F_2 mode splits into three features: a unit δ function at ω_3, another at ω_4, and a band of unit area between them.

The parameters used in creating Fig. 2 are approximately those that I will deduce for vitreous (v-) SiO_2, including $\theta(SiO_2) \simeq 130°$. Therefore, inspection of the distribution of states depicted by the lower set of dashed lines ($\theta = 130°$) reveals the extensive departures from the prediction of an isolated-molecule model ($\theta = 90°$) that are caused by the intertethedral coupling of bond-stretching forces at angles θ typical of oxide glasses. Isolated molecule models are inadequate.

To relate these results to experimental spectra, I argue as follows. It is known that the intertetrahedral angle in real glasses is not everywhere the same, but is distributed about some most likely value, estimated by x-ray diffraction to be 144° in v-SiO_2,[4] 133° in v-GeO_2,[5] and 146° in v-BeF_2.[6] I approximate the true situation with an ensemble of local environments, each as shown in Fig. 1, with disorder accounted for by a statistical distribution of the angle θ used in Eqs. (1)–(4). The resultant statistical distribution of local densities of states will lead to a *total* density of states related to that shown in the lower part of Fig. 2, with the difference that both the bands and the δ functions will be broadened, and *the latter will dominate*. That is, if one ascribes to each δ function a width of the order of a phonon natural linewidth (say 1 cm^{-1}) and anticipates the result that the separation $\omega_4 - \omega_2$ for v-SiO_2 is about 200 cm^{-1}, one concludes that for reasonable spreads in θ (say ±10°) the total density of states will be dominated by bands due to the distribution of δ-function contributions. I therefore associate the center of the two highest-frequency bands seen in these glasses with ω_3 and ω_4, evaluated at the most probable intertetrahedral angle.[7]

Sen and Thorpe also associated ω_3 and ω_4 with certain features of reported spectra, but they made no detailed study of the accuracy of their formulas, nor did they report any use for the other two frequencies ω_1 and ω_2. I shall address both of these subjects.

II. ACCURACY OF THE MODEL

An obvious use of Eqs. (3) and (4) is to solve them for α and $\cos\theta$ in terms of the experimentally determined values $\omega_3 = \omega_3(\theta)$ and $\omega_4 = \omega_4(\theta)$:

$$\alpha = \tfrac{1}{2}(\omega_3^2 + \omega_4^2) m_X (1 + 4m_X/3m_A)^{-1} , \qquad (5)$$

$$\cos\theta = (\omega_3^2 - \omega_4^2)(\omega_3^2 + \omega_4^2)^{-1}(1 + 4m_X/3m_A) . \qquad (6)$$

These expressions involve the assumption that $\beta = 0$, so it is instructive to test them against the more accurate large-cluster computations of Bell, Dean, and Hibbins-Butler (BDH),[8] who used $\beta \simeq 0.18\alpha$. The results are contained in the first six columns of Table I for the three materials that BDH considered. In Table I, W_3 and W_4 are the central wave-number values of the two highest-frequency peaks in the total density of states computed by BDH, θ and α are computed from these using Eqs. (5) and (6), and α_{BDH} is the bond-stretching force constant input to their calculations by BDH. It is quite encouraging that the computed values of θ are essentially the same, and are only ~10% less than 140°, the mean A-X-A angle for the model structure that BDH used for all three materials.[9] It is similarly encouraging that the computed values of α are only about 10% higher than those input by BDH.

It is also possible to obtain good estimates of the noncentral force constant β by direct calculation from the position of a feature in the low-freq-

TABLE I. Test of Eqs. (5)–(7), using W_3, W_4, and W_0 from the theoretical density of states of Bell, Dean, and Hibbins-Butler (BDH) as input. Note that derived values of θ, α, and β are within ~10% of the BDH values ($\theta_{BDH} \simeq 140°$). W is in units of cm^{-1}, and α and β in N/m.

AX_2	W_3	W_4	$\theta°$	α	α_{BDH}	W_0	β	β_{BDH}
SiO_2	740	1050	126	444	(400)	420	79	(71)
GeO_2	500	845	128	354	(330)	375	67	(58)
BeF_2	620	725	126	134	(110)	190	20	(19)

uency portion of the vibrational spectra. In this case, I build upon a result reported by Kulas and Thorpe (KT),[10] who successfully used an effective-medium approach to calculate the density of states of a hypothetical AX_2 glass with *straight* A-X-A bonds ($\theta \equiv 180°$), for the case that *both* α and β are nonzero. They obtain a δ function at a low frequency ω_o given by $\omega_o^2 = 2\beta/m_X$. This frequency corresponds to motion of the X atoms in a direction perpendicular to the A-X-A line, without motion of the A atoms and with negligible stretching of either A-X bond, conditions that are reflected by the absence from this equation of m_A and α, respectively. Some of these properties are retained by the "rocking" motion R in Fig. 1 as θ departs from 180°, so it seems reasonable to expect a δ function in the density of states to persist near ω_0 at a frequency only weakly dependent on θ. I therefore explore the determination of β from the simple expression

$$\beta \simeq \tfrac{1}{2}\omega_o^2 m_X . \tag{7}$$

When this formula is tested against the exact calculations of BDH, as shown in the last three columns of Table I, the derived values of β are found to be remarkably clost to the input values β_{BDH}. While the exact atomic motion involved is uncertain, it is evident that Eq. (7) yields useful values of β (on the order of 10% too large).

From this analysis, I conclude that Eqs. (1)–(7) yield quantities that are within ~10% of those given by an essentially exact calculation based on Born forces and realistic disorder (the BDH calculations). This shows remarkable accuracy, considering the apparent complexity of the vibrational system and the mathematical simplicity of Eqs. (1)–(7). To the extent that the BDH theory is applicable to real glasses (especially v-SiO$_2$, v-GeO$_2$, and v-BeF$_2$), this quantitative success encourages the use of Eqs. (1)–(7) in interpreting observed spectra.

III. APPLICATION TO REAL GLASSES: v-SiO$_2$, v-GeO$_2$, and v-BeF$_2$

Application of these expressions to real experimental data uncovers a new difficulty—owing to the known splitting of the highest-frequency mode into a well-separated transverse-optical–longitudinal-optical (TO-LO) pair.[7] The problem is the absence of a good theory for predicting the position of the so-called bare mode, whose frequency is split by Coulomb interactions into a TO-LO pair. We have argued elsewhere[2,11] that the bare mode lies nearer the LO frequency than the TO frequency in v-SiO$_2$, v-GeO$_2$, and v-BeF$_2$, and results to be presented later in this paper strongly support this assertion.

TABLE II. Application of Eqs. (1), (2), (5), and (6) to experimental LO frequencies W_3 and W_4. θ_X is the x-ray estimate. Note the close correspondence of computed W_1 to the observed Raman frequency W_R. Units are as in Table I.

AX_2	W_3	W_4	α	θ°	θ_X°	W_2	W_1	W_R
SiO$_2$	820	1200	569	130	144	992	464	(450)
GeO$_2$	595	973	478	126	133	894	455	(420)
BeF$_2$	810	940	227	124	146	562	297	(295)

Thus, I tentatively applied Eqs. (5) and (6) to the experimentally observed LO values of W_3 and W_4, taken from Refs. 7 and 11. The results are tabulated in Table II. The values of θ are about 10% less than those deduced from diffraction studies (θ_X),[4-6] while those for α are presumably ~10% too high, as in Table I. Use of these quantities in Eqs. (2) and (1) leads to the values of W_2 and W_1 given in Table II, and comparison of the last two columns reveals an important new result.

A. Origin of the dominant Raman line (W_1)

The wave-number value W_1 of the derived lowest-frequency limit ω_1 is remarkably close in each case to the observed position W_R of the main peak in the Raman spectrum. From this, I infer that the dominant peak in the Raman spectrum occurs *at the low-frequency edge* of the band whose parentage is the breathing mode of the isolated molecule, and that the Raman matrix element (or coupling coefficient) must peak sharply at this position ($\approx W_1$). This is an extremely interesting result, demonstrating a case where a coupling coefficient in the theory of Shuker and Gammon[12] is *not constant*, but is a sharp function of frequency over the band involved,[13] and peaks near one edge.

The Raman selection rule is most easily understood as follows. First, one notes that according to ST, ω_1 corresponds to pure "bending" motion of the X atom, as defined by B in Fig. 1, without any motion of the A atoms. This involves a simultaneous stretching of two neighboring A-X bonds, as opposed to the situation in an S motion in Fig. 1, where the stretching of one bond results in the compression of its immediate neighbor. Since Raman scattering in related materials is known to arise largely from changes in bond length rather than bond angle,[14] we imagine that Raman strength is maximum for the in-phase stretching associated with B motion at ω_1, and is greatly reduced for the out-of-phase stretching associated with S motion, which occurs in pure form at the ω_2 band edge. The *enhancement* of Raman activity when neighboring bonds are compressed in phase, and the *reduction* when some bonds are compressed while others are extended, is well known in studies of molecules, and is given an elegant elementary discussion in the textbook by Long.[15]

B. Minimization of the TO-LO problem

Since the main Raman line is infrared (IR) inactive, it has no observable TO-LO splitting, and its frequency ($\omega_R \rightarrow \omega_1$) can be used to deduce α and θ, thereby avoiding the ambiguity raised by the large TO-LO splitting of ω_4. Since ω_3 has little TO-LO splitting, it is advantageous to retain use of this feature. The required solution of Eqs. (1) and (3) is

$$\alpha = (\omega_2^2 - \omega_1^2)\tfrac{3}{4} m_A \,, \tag{8}$$

$$\cos\theta + 1 = \frac{\omega_1^2}{\omega_3^2 - \omega_1^2}\,\frac{4m_X}{3m_A}. \tag{9}$$

The result of applying these equations to the experimental data is shown in Fig. 3 and the first six columns of Table III. The values of α and θ are the best obtained by this type of analysis, although they will be improved if $\beta \neq 0$ can be included in the formalism. In Fig. 3 one sees that with $W_1 = W_R$ and W_3 as input, the derived value of the bare-mode frequency W_4 (cm^{-1}) always lies between the high-frequency TO-LO pair, and closer to the LO than the TO peak. In contrast, W_2 fails to correspond consistently to any Raman or infrared spectral feature.

C. Estimation of the noncentral force constant

The noncentral force constant β is extracted from the data using Eq. (7), with ω_0 identified as the lowest-frequency peak in the IR spectrum of ε_2. (This IR-active line does not show in any of the Raman spectra of Fig. 3, but may be seen in the ε_2 spectra of Refs. 7 and 11; its frequency accidentally coincides with that of the main Raman peak in v-SiO$_2$, but not in v-GeO$_2$ and BeF$_2$.) The resultant values of β and β/α are tabulated in the last two columns of Table III, where it can be seen that the value of β/α used by BDH (0.18) was excellent for v-SiO$_2$, about twice *too large* for v-GeO$_2$, and twice *too small* for v-BeF$_2$. According to this analysis, recalculation of the BDH densities of states using the values of β/α in Table III should improve the comparison between their theory and the experimental results for v-GeO$_2$ and v-BeF$_2$.

D. Spread in intertetrahedral angle θ

The present model can be used to estimate the spread in θ. This is done by ascribing the width

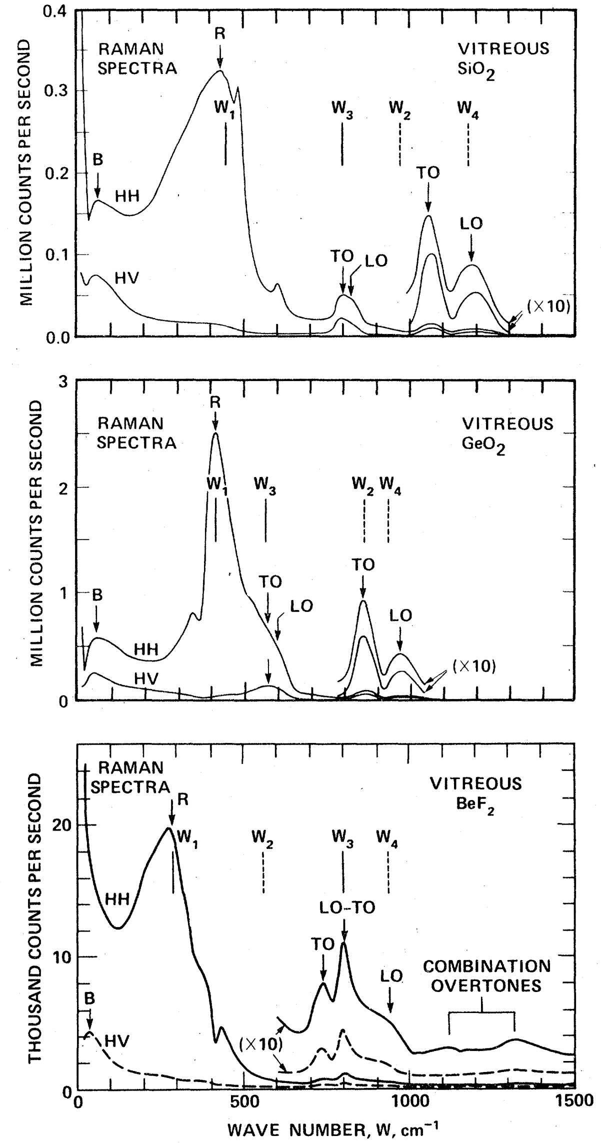

FIG. 3. Comparison of the present analysis with the Raman spectra of vitreous SiO$_2$, GeO$_2$, and BeF$_2$. The solid vertical lines mark frequencies W_1 and W_3 which are input to the analysis, while the dashed vertical lines are output. Note that W_4 always lies just below the high-frequency LO line, while W_2 does not consistently correspond to any spectral feature.

TABLE III. Application of Eqs. (7)–(9) to the experimental TO frequencies $W_1 \equiv W_R$, W_3, and W_0 (see also Fig. 3). Note that the BDH value for β/α (0.18) is excellent for SiO$_2$, but appears to be too large for GeO$_2$ and too small for BeF$_2$. Units are as in Table I.

AX_2	W_R	W_3	$\theta°$	α	W_4	W_0	β	β/α
SiO$_2$	450	800	130	545	1176	455	98	0.17
GeO$_2$	420	556	128	431	930	278	37	0.08
BeF$_2$	295	810	125	228	941	400	90	0.40

of the observed spectral lines entirely to the width of an assumed peak in the distribution of θ. Although this approach is clearly oversimplified, since it does not account for effects due to dihedral angles or variations of force constants with θ, it appears to give reasonable results, and may correctly predict which materials actually have greater spread in θ.

For small variations $\Delta\theta$, the change $\Delta\omega_i$ in any one of the frequencies ω_i $(i=1,2,3,4)$ is given by

$$\omega_i \Delta\omega_i = \gamma_i(\alpha/2m_X)\sin\theta\,\Delta\theta\ , \tag{10}$$

where $\gamma_x = -1$ $(i=1,3)$ and $\gamma_i = +1$ $(i=2,4)$. These equations are obtained by differentiation of Eqs. (1)–(4) under the simplifying assumption that α is independent of θ. The results of applying Eq. (10) to v-SiO_2, v-GeO_2, and v-BeF_2 are given in Table IV, where $\Delta\theta_i$ is the angular spread required to account for the observed full width at half maximum (FWHM) ΔW_i of the three principal bands $W_1 = W_R$, W_3, and W_4. The center wave-number values W_i and the corresponding values of α and θ are taken from Table III. Where possible, the linewidths are estimated from the Raman spectra in Fig. 3; otherwise they are obtained from the reduced Raman spectra (or the IR ε_2 spectra) in Refs. 7 and 11. For ΔW_4 I have used the width of the LO mode, which is clearly wider than the TO band in v-SiO_2 and v-GeO_2 (cf. Fig. 3).

The trends are as follows. For each material, the $\Delta\theta_i$ vary among themselves by a factor of about 2. If the model were adequate to determine $\Delta\theta$, the values of $\Delta\theta_i$ would be essentially the same. In particular, $\Delta\theta_4$ is always larger than $\Delta\theta_3$ or $\Delta\theta_1$, and this may be partly due to unknown broadening effects of the neglected long-range forces that give rise to the pronounced TO-LO splitting of W_4. On other other hand, in v-SiO_2 (where data are available) the x-ray estimate of $\Delta\theta$ is ~35°,[4] rather close to the presently derived value $\Delta\theta_4 \sim 34°$. It is also true that only in v-GeO_2 is $\Delta\theta_1$ smaller than $\Delta\theta_3$; this exception may be associated with the small value of β/α deduced for v-GeO_2, and may therefore signal the need for inclusion of noncentral forces or a special distribution of dihedral angles in order to better explain linewidths. In general, the calculated angular spreads are greatest for v-BeF_2 and smallest for v-GeO_2. It is my suspicion that both the present estimates and the x-ray estimates suffer from the unrealistic assumption that there are no preferred dihedral angles.

IV. CONCLUDING REMARKS

From a study of the present analysis and related ones given in Refs. 1 and 2, the following generalizations can be made. They are true for AX_2 tetrahedral glasses and should be approximately true for nontetrahedral glasses based on 2-coordinated bridging (X) atoms. First, the dominant Raman peak will involve motion of the X atom along a line bisecting the A-X-A angle, the B motion in Fig. 1.[16] I prefer to call this a *symmetric-stretch* (SS) motion, since when acting alone it results in identical distortion of the two neighboring A-X bonds. Second, the highest-frequency IR-active mode will involve motion of the X atom along a line parallel to A-A, the line between the bridged atoms. This is the S motion in Fig. 1, which I suggest be called an *antisymmetric-stretch* (AS) motion, since it results in opposite distortions of the two neighboring A-X bonds. Third, the next lower frequency IR-active mode will involve SS motion of the X atom, but here as in the higher-frequency IR mode there is a substantial amount of A-atom motion depending on the ratio of the masses m_X/m_A, the average θ, and the coordination of the cation (A atom). Fourth, the lowest-frequency IR-active mode will primarily involve rocking motion of the bridging atom, as defined by R in Fig. 1, but again including some cation motion. Some of these modes may be split in glasses where the A atom is not tetrahedrally coordinated.

Further explorations of the use of the band limits are underway. These involve an analysis of v-GeS_2, v-$GeSe_2$, and v-$ZnCl_2$ as well as calculations for other glass structures, including those appropriate for v-P_2O_5, v-As_2O_3, and v-B_2O_3. In the case of v-$GeSe_2$, I have found no way for the present theory to account for *both* of the strong Raman peaks reported by Nemanich *et al.*[17] I conclude that v-$GeSe_2$ contains some structural elements not inherent in the network underlying the ST calculations.

In summary, the present paper has developed simple procedures for extracting useful values of the central and noncentral force constants and the most probable intertetrahedral angle from the Raman and infrared spectra of AX_2 tetrahedral

TABLE IV. Investigation of the spread in intertetrahedral angle $\Delta\theta_i$ required to account for the observed linewidth ΔW_i (FWHM) of the principal bands W_i in the Raman spectra of v-SiO_2, v-GeO_2, and v-BeF_2. The spreads are largest for v-BeF_2 and (except for $\Delta\theta_3$) smallest in v-GeO_2. Units are as in Table I.

AX_2	ΔW_1	$\Delta\theta_1^\circ$	ΔW_3	$\Delta\theta_3^\circ$	ΔW_4	$\Delta\theta_4^\circ$
SiO_2	200	23	75	15	110	34
GeO_2	100	13	100	18	80	26
BeF_2	160	33	40	22	60	41

glasses. Equations (7)–(9) were derived from a central force network model which was shown to give the same values as a more exact large-cluster calculation to within 10%. Application to the spectra of v-SiO_2, v-GeO_2, and v-BeF_2 revealed that the dominant Raman peak in those materials is due to a matrix-element effect and involves a symmetric stretch of the A-X bonds in phase with one another. These results demonstrate the practical and heuristic value of the calculations of Sen and Thorpe,[1] and suggest that extensions of their method will be worthwhile.

ACKNOWLEDGMENTS

I am grateful to Dr. R. M. Martin, Dr. P. N. Sen, and Professor M. F. Thorpe for helpful discussions during portions of this work.

---

[1] P. N. Sen and M. F. Thorpe, Phys. Rev. B 15, 4030 (1977); for a review of large-cluster calculations including noncentral forces, see R. J. Bell, in *Methods in Computational Physics*, edited by G. Gilat (Academic, New York, 1976), p. 215; for an example of cluster Bethe-lattice calculations including noncentral forces, see R. B. Laughlin and J. D. Joannopoulous, Phys. Rev. B 16, 2942 (1977).

[2] See also F. L. Galeener, in *Lattice Dynamics*, edited by M. Balkanski (Flammarion, Paris, 1978), p. 345; Bull. Am. Phys. Soc. 23, 338 (1978).

[3] R. J. Bell and P. Dean, Discuss. Faraday Soc. 50, 55 (1970).

[4] R. L. Mozzi and B. E. Warren, J. Appl. Crystallogr. 2, 164 (1969).

[5] A. J. Leadbetter and A. C. Wright, J. Non-Cryst. Solids 7, 37 (1972).

[6] This uncertain value was reported by A. J. Leadbetter and A. C. Wright, J. Non-Cryst. Solids 7, 156 (1972).

[7] In several AX_2 glasses the highest-frequency mode is split into a TO-LO pair as first demonstrated by F. L. Galeener and G. Lucovsky, Phys. Rev. Lett. 37, 1474 (1976). A theory for the splitting has been proposed by R. M. Pick and M. Yvinec in Ref. 2, p. 459.

[8] R. J. Bell, P. Dean, and D. C. Hibbins-Butler, J. Phys. C 3, 2111 (1970).

[9] R. J. Bell and P. Dean, in *Proceedings of the International Conference on Localized Excitations in Solids*, edited by R. F. Wallis (Plenum, New York, 1968), p. 124.

[10] R. Kulas and M. F. Thorpe, in *Structure and Excitations of Amorphous Solids* (American Institute of Physics, New York, 1976), p. 251.

[11] F. L. Galeener, G. Lucovsky, and R. H. Geils, Solid State Commun. 25, 405 (1978).

[12] R. Shuker and R. W. Gammon, Phys. Rev. Lett. 25, 222 (1970).

[13] For a theoretical discussion, see F. L. Galeener and P. N. Sen, Phys. Rev. B 17, 1928 (1978).

[14] D. A. Kleinman and W. G. Spitzer, Phys. Rev. 125, 16 (1962).

[15] D. A. Long, *Raman Spectroscopy* (McGraw-Hill, New York, 1977), p. 65ff.

[16] In v-P_2O_5 this peak is somewhat weaker than a higher-frequency Raman mode due to P=O double bonds: F. L. Galeener and J. C. Mikkelsen, Jr., Solid State Commun. (to be published).

[17] R. J. Nemanich, S. A. Solin, and G. Lucovsky, Solid State Commun. 21, 273 (1977).